


Electrophysiological patterns and structural substrates of Brugada syndrome: Critical appraisal and computational analyses

Paolo Seghetti MSc^{1,2} | Sara Latrofa MSc¹ | Niccolò Biasi PhD³  | Alberto Giannoni MD, PhD^{1,4} | Valentina Hartwig PhD^{2,4} | Andrea Rossi MD⁴ | Alessandro Tognetti PhD^{3,5}

¹Health Science Interdisciplinary Center, Scuola Superiore Sant'Anna, Pisa, Italy

²Institute of Clinical Physiology, National Research Council, Pisa, Italy

³Department of Information Engineering, Università di Pisa, Pisa, Italy

⁴Fondazione Toscana 'G. Monasterio', Pisa, Italy

⁵Research Center 'Enrico Piaggio', Università di Pisa, Pisa, Italy

Correspondence

Paolo Seghetti, MSc, Sant'Anna School of Advanced Studies, Pisa, Italy.

Email: p.seghetti@santannapisa.it

Disclosures: None.

Abstract

Brugada syndrome (BrS) is a cardiac electrophysiological disease with unknown etiology, associated with sudden cardiac death. Symptomatic patients are treated with implanted cardiac defibrillator, but no risk stratification strategy is effective in patients that are at low to medium arrhythmic risk. Cardiac computational modeling is an emerging tool that can be used to verify the hypotheses of pathogenesis and inspire new risk stratification strategies. However, to obtain reliable results computational models must be validated with consistent experimental data. We reviewed the main electrophysiological and structural variables from BrS clinical studies to assess which data could be used to validate a computational approach. Activation delay in the epicardial right ventricular outflow tract is a consistent finding, as well as increased fibrosis and subclinical alterations of right ventricular functional and morphological parameters. The comparison between other electrophysiological variables is hindered by methodological differences between studies, which we commented. We conclude by presenting a recent theory unifying electrophysiological and structural substrate in BrS and illustrate how computational modeling could help translation to risk stratification.

KEYWORDS

Basic: Computer modeling/simulations, Basic: Ventricular tachycardia/fibrillation, Clinical: Cardiac mapping – electrogram analysis, Clinical: Electrophysiology – Brugada syndrome, Clinical: Electrophysiology – cardiac arrest/sudden death

1 | INTRODUCTION

Brugada syndrome (BrS) is a cardiac electrophysiological disease characterized by an increased risk of sudden cardiac death (SCD) and a specific ECG pattern of ST-segment elevation followed by a negative T-wave in at least one right precordial lead ("type 1" ECG pattern). Typical symptoms of BrS patients are syncope, agonal nocturnal respiration, palpitation, and SCD. Every year, up to 0.5%–1% of asymptomatic BrS patients present an arrhythmic event

due to ventricular fibrillation (VF) or ventricular tachycardia (VT),^{1–3} with most patients presenting their first arrhythmic event between 38 and 48 years of age.⁴ The current standard of care for BrS patients is the implantable cardioverter defibrillator (ICD). ICD is strongly recommended for symptomatic BrS patients with previous cardiac arrest (class I indication), whereas ICD implantation in primary prevention indication is still debated (class IIa indication).⁵ Recently, the epicardial ablation of the arrhythmogenic substrate located in the right ventricular outflow tract (RVOT) has been proposed as an

alternative therapeutic solution in selected cases (class IIa indication).⁵⁻⁷ Recent trials showed a low recurrence of events after complete elimination of the arrhythmogenic substrate.^{6,8,9} To date, one of the main challenges in BrS is the risk stratification of asymptomatic patients: eight multifactor risk scores have been proposed,¹⁰ however, their predictive value for intermediate risk groups is limited (median AUC using ROC curves 0.531, maximum AUC 0.7).¹⁰⁻¹² Furthermore, the low rate of events in asymptomatic patients and the duration of follow-up make it so that only strongly predictive variables can be used as reliable risk factors when using an event-driven approach. In clinical practice, programmed ventricular stimulation (PVS) is the only widely used tool for risk stratification, even though its sensitivity and specificity in predicting VF has been questioned.^{2,3,13,14} Recently, it has been shown that PVS can be used to distinguish between high-risk and low-risk asymptomatic patients in selected cohorts of patients,^{15,16} however it is not suitable for mass screening and both sensitivity and specificity of the test depend on the PVS protocol used.^{16,17} Several electroanatomical mapping (EAM) studies showed that the RVOT of BrS patients is characterized by the presence of low amplitude, fractionated electrograms (EGMs), and conduction slowing. However, the nature of these abnormalities is debated. The two main theories describing arrhythmogenesis in BrS are the repolarization and the depolarization hypotheses. The repolarization hypothesis was proposed by the group of Antzelevitch from observations on wedges of canine hearts treated pharmacologically to replicate the phenotype of BrS. The group observed that the BrS phenotype was caused by a prominent repolarization notch during phase 1 of the AP, which determined either a prolongation of AP duration or, in extreme cases, early repolarization of the myocyte (i.e., loss of AP dome); responsible for phase 2 reentrant arrhythmias.¹⁸⁻²⁰ The depolarization hypothesis states that localized slow ventricular conduction is the basis for the phenotype and arrhythmogenesis of the syndrome. Conduction slowing would be caused by structural factors in the RVOT, such as diffuse fibrosis or reduced connexin-43 expression, being responsible for the presence of fractionated EGMs and low voltage areas.²¹ Even though there is a

relative abundance of data concerning the electrophysiology of BrS patients, their quantitative values are rarely compared between studies, and a clear range of variability is not defined. The determination of clear ranges for electrophysiological parameters could allow mathematical modeling of the electrophysiological basis of BrS. Furthermore, a definition of the electrophysiological parameters involved in BrS and their quantitative value could help check which features are involved in arrhythmogenesis. Therefore, this work aims to review and comment on the clinical and experimental electrophysiological data available in the literature regarding BrS patients to define better the BrS electrophysiological substrate, in the perspective of improving risk stratification. We divide data into two categories, electrophysiological and structural, and comment on each section with what can be considered solid or uncertain evidence.

2 | RESULTS FROM ELECTROPHYSIOLOGICAL STUDIES

2.1 | Methods to estimate action potential duration (APD)

APD can be estimated from signals recorded on the cardiac surface either from unipolar electrograms (UEGs) or from monophasic action potentials (MAPs). The MAP procedure replicates the myocyte action potential (AP) by applying significant pressure on the ventricular wall with the catheter during recording.^{22,23} In this case, the APD can be estimated directly from the recorded signal without additional processing. To estimate APD from UEGs, the activation recovery interval (ARI) can be calculated; this interval is measured from the activation time (time of minimum derivative of the UEG signal) to the repolarization time (time of maximum derivative during the local T wave), and correlates with the APD²⁴⁻²⁶ (refer to Figure 1). ARIs can be computed either directly from UEGs measured from mapping catheters or from UEGs reconstructed using the ECGI methodology, which solves a mathematical problem from measures on the patient's

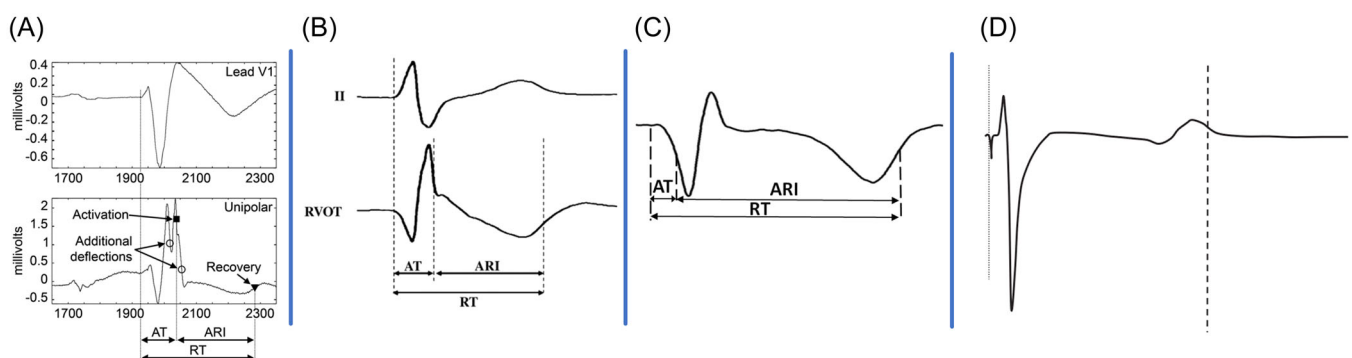


FIGURE 1 Different unipolar electrograms measured in different recording setups. Note that the methodology of acquisition influences the number and amplitude of deflections during local depolarization. (A) endocardial UEG recording from Postema et al.²⁷; (B) endocardial UEG recording from Nagase et al.²⁸; (C) representative epicardial UEG computed with the ECGI technique from Zhang et al.²⁹; (D) epicardial UEG computed in an explanted porcine heart in the study by Coronel et al.²⁶

torso.³⁰ Several experimental and computational studies showed the correspondence of minimal deflection in the ventricular UEG with local depolarization. The same studies demonstrated that, when assessing local repolarization, the maximum positive derivative of the T wave is the best hallmark of local repolarization.^{24–26} Despite such theoretical background, computed ARIs are different between studies (Table 1). As illustrated in Figure 1, UEGs can have different morphologies with more than one steep negative deflection, each possibly indicating local depolarization. We report some explanatory examples: in Figure 1D it is clear which deflection corresponds to local depolarization; if we consider Figure 1A–C, each negative deflection could represent partial/discontinuous local depolarization. In this case, the most correct method would be to consider the last deflection, as proposed by Nademanee et al.,³⁷ or to consider deflections in the local bipolar EGM. Finally, UEGs computed from ECGI studies, as the one reported in Figure 1C,²⁹ usually are smoother due to the low pass action of biological tissues; this might determine a lower number of deflections in UEGs and, therefore, a bias in the identification of activation time. Regarding the end of local repolarization, studies demonstrated that the most robust indicator is the maximum derivative of the T-wave, irrespective of its polarity.^{24,26} However, using the T-wave to estimate local repolarization is prone to systematic errors that depend on the measurement and filtering setup^{25,38} (e.g., electrode dimension and electrode-tissue distance). Therefore, further studies are needed to assess the reliability and robustness of each acquisition method in an *in vivo* setting and to estimate the relation between results obtained using different techniques.

2.2 | Estimated action potential duration (eAPD)

Studies adopting the MAP procedure^{31–33} yield consistent results, with an estimated endocardial APD of ≈230 ms, whereas ARI studies^{27,28,34} estimated longer and more dispersed APD. Overall, ECGI studies^{29,35,36} had the longest estimate of APD. No study found a significant difference in endocardial eAPD between BrS patients and controls, even though there is a trend toward reduced endocardial ARI in BrS patients versus controls in the studies of Postema et al.²⁷ and Nagase et al.²⁸ Only two studies measured APD differences between epicardial and endocardial layers in BrS patients, however, the differences identified were not statistically significant at baseline, and only modest after pharmacological challenge.^{28,35} The same studies reported that sodium-channel blockade challenge increased epicardial ARI duration, whereas its effect on the endocardium was nonsignificant.^{28,35} Considering these studies,^{28,35} ajmaline challenge seems to prolong the epicardial APD while having no effect on the endocardial layer. However, Pannone et al.³⁶ found that ajmaline shortened epicardial APD in patients with aborted SCD, whereas it had no effect on the non-SCD group. The discrepancy in this result may be caused by the different methodologies used to acquire cardiac signals, which likely have different sensitivity to epicardial and endocardial potentials (EAM Nagase et al.,²⁸ ECGI

Pannone et al.,³⁶ epi-endo ECGI Rudic et al.³⁵). Of note, several studies measured the effective refractory period (ERP) in the endocardium of BrS patients, however, only Ashino et al.³¹ found a significant difference between patients and controls.^{27,32,33,39} To date, there are three studies that reproduced a consistent AP shape of BrS myocytes. A postmortem case report⁴⁰ and a Human induced Pluripotent Stem Cells (HiPSC) study⁴¹ did not find overt differences in APD between BrS myocytes and healthy myocytes, differently from what was obtained by Kurita et al.⁴² using *in vivo* measures in three BrS patients. Importantly, all three studies found a similar AP shape: a reduced phase 1 upstroke and a prominent AP dome. Furthermore, several studies found altered APD restitution properties in BrS patients,^{31–33} and Aras et al.⁴³ demonstrated a shorter APD in the healthy human heart RVOT when compared with the right ventricular apex (RVA). The implications of these findings have not been explored yet. In conclusion, the measurement of APD in BrS has yielded contradicting results in studies so far. Evidence rather suggests that AP shape and restitution properties might have a relevant role in the pathogenesis and phenotype of BrS.

2.3 | Depolarization, activation time, and fractionation

The alteration of the depolarization dynamics in BrS patients is supported by the presence of conduction delay, isochronal crowding, and EGMs fractionation in the RVOT evidenced by numerous studies. There is solid evidence about conduction delay in the epicardial RVOT of BrS patients. On the contrary, the activation pattern on the endocardial side is not clearly defined, but the presence of a type 1 ECG pattern seems to be related to prolonged AT. Even though activation delay in the epicardial RVOT of BrS patients is well established, its prolongation is not statistically significant when considering baseline BrS patients compared with controls. However, the ECGI study from Zhang et al.,²⁹ the endocardial EAM studies of Lambiase et al.,⁴⁴ and Postema et al.,²⁷ identified crowding of isochrones and activation delay in specific areas of the RVOT when compared with the rest of the right ventricle (RV). This regional variability in ATs is probably the reason why AT reported as mean and standard deviation, as in most studies, is not a good discriminant between BrS patients and controls. As can be noted considering the mean values from Table 2, endocardial EAM studies that considered only the RVOT found higher AT values than epicardial studies that considered the whole RV, which is in contrast with the notion that the late activating substrate of BrS is located in the epicardium. Moreover, studies that considered the RVOT AT found statistical significance between the AT of type 1 BrS patients and type 2 or controls,^{27,44,45} indicating that BrS patients with a normal or type 2 ECG at the time of study do not have an altered activation pattern. The few studies that systematically investigated the effect of ajmaline on the RV AT reported that it increased the area of delayed activation and overall AT,

TABLE 1 Estimated APD from different studies.

References (n° of patients)	Epicardial estimated APD (ms)	Endocardial estimated APD (ms)	Epicardial estimated APD challenge (ms)	Endocardial estimated APD challenge (ms)
Ashino et al. ³¹				
[MAP]				
BrS RVOT (16)		226.6 ± 15.5		
Control RVOT (17)		233.9 ± 15.9		
Ashino et al. ³²				
[MAP]				
BrS RVOT G1 (6)		225.3 ± 9.2		
BrS RVOT G2(3)	-	228.3 ± 31.5	-	-
Nishii et al. ³³				
[MAP]				
BrS RVOT (39)		242 ± 14		
Control RVOT (9)		242 ± 11		
BrS RVA (39)		237 ± 15		
Control RVA (9)	-	232 ± 20	-	-
Hayashi et al. ³⁴				
[EAM]				
BrS RVOT (21)		286 ± 18		
BrS RVA (21)	-	286 ± 19	-	-
Nagase et al. ²⁸				
[EAM]				
BrS (19)	223 ± 16	219 ± 17	235 ± 22	214 ± 17
Control (3)	239 ± 15	256 ± 13	227 ± 14	245 ± 16
Postema et al. ²⁷				
[EAM]				
BrS type 1 (9)		248 ± 20		
BrS type 2 (10)		250 ± 10		
Control (9)	-	270 ± 5	-	-
Rudic et al. ³⁵				
[ECGI]				
BrS type 1 (6)	281 ± 34	297 ± 13		
BrS type 2 (6)	247 ± 50	262 ± 60	323 ± 43	311 ± 68
Control (15)	247 ± 26	271 ± 51	-	-
Zhang et al. ²⁹				
[ECGI]				
BrS RVOT (25)	318 ± 32			
BrS RVA (25)	221 ± 37			
Pannone et al. ³⁶				
[ECGI]				

TABLE 1 (Continued)

References (n° of patients)	Epicardial estimated APD (ms)	Endocardial estimated APD (ms)	Epicardial estimated APD challenge (ms)	Endocardial estimated APD challenge (ms)
RVOT SCD (12)	301.5 ± 31.2		270.7 ± 32.3	
RVOT non SCD (27)	299.2 ± 38.7	-	309.4 ± 41.6	-

Note: Each study used different methodologies, however, the estimated values are similar. Different acquisition techniques are marked in square brackets. Results are as mean ± standard deviation.

TABLE 2 Right ventricle activation times from different clinical studies.

References (n° of patients)	Epicardial RVAT (ms)	Endocardial RVAT (ms)	Epicardial RVAT challenge (ms)	Endocardial RVAT challenge (ms)
Lambiase et al. ⁴⁴				
[EAM]				
BrS (18)		125 ± 10		
Nagase et al. ²⁸				
[EAM]				
BrS (19)	86 ± 15	77 ± 16	111 ± 25	98 ± 25
Control (3)	73 ± 16	67 ± 15	91 ± 6	87 ± 6
Postema et al. ²⁷				
[EAM]				
BrS type 1 (9)		117 ± 8		
BrS type 2 (10)		85 ± 4		
Control (9)	-	81 ± 2	-	-
Letsas et al. ⁴⁵				
[EAM]				
BrS (10)		87.3 ± 16.4		
Control (20)	-	63.8 ± 9.8	-	-
Pannone et al. ³⁶				
[ECGI]				
RVOT SCD (12)	65.0 ± 31.9		138.1 ± 17.7	
RVOT non SCD (27)	66.2 ± 22.2	-	91.6 ± 24.9	-
Rudic et al. ³⁵				
[ECGI]				
BrS G1 (6)	65 ± 19	65 ± 20		
BrS G2 (6)	60 ± 9	53 ± 7	78 ± 12	85 ± 20
Control (15)	50 ± 13	38 ± 13	-	-
Zhang et al. ²⁹				
[ECGI]				
BrS (25)	82 ± 18	-	-	-

Note: Different acquisition techniques are marked in square brackets. Results are as mean ± standard deviation.

sometimes causing conduction block in the center of the delayed area.^{37,46,47} To summarize, the presence of a type 1 ECG and the selection of AT based on the anatomical district both severely affect the statistical significance of the comparison between BrS patients and controls. The presence of abnormal fractionation in bipolar EGMs is found reliably in a well-defined region in the epicardial substrate. Epicardial EGMs fractionation duration ranges from 76 ± 28 ms found by Nademanee et al.^{4,7} to 230 ms reported by the group of Pappone⁷ and is found in a well-defined area in the epicardial RVOT. High-frequency pacing or ajmaline challenge causes prolongation of EGM fractionation and even conduction block in the RVOT epicardium.^{37,46,47} Only a few studies identified regions in the RVOT endocardium presenting with abnormal EGMs, and the effects of ajmaline on the endocardium are seldom studied. In the endocardium, the reported fractionation duration is shorter and the affected area is more scattered when compared with the epicardial layer (Table 3).^{27,44,45} A recent study conducted by Letsas et al.⁴⁸ demonstrated that fractionated, low-voltage areas detected in bipolar epicardial mapping corresponded to low-voltage areas in endocardial unipolar mapping. The extension of the endocardial

low voltage area could discriminate between symptomatic and asymptomatic patients.⁴⁸ The variability among fractionation duration in studies may be caused by different definitions of fractionation in EGMs, determined by the presence of multiple deflections in the signal,²⁷ low voltage amplitude deflections after the QRS,⁴⁸ prolonged EGM duration,⁷ or a combination of the above.^{37,46,49} In addition to different evaluation metrics, different techniques are used for signal acquisition, different anatomical locations are examined (epicardial or endocardial, RVOT or whole RV), and different thresholds are used to distinguish between normal and abnormal EGMs that are considered for duration measurement. Studies that performed both epicardial and endocardial mapping did not identify a pathological substrate on the endocardial side.^{7,37,46} To conclude, both endocardial and epicardial EAM studies and ECGI studies confirmed that the presence of a type 1 ECG is associated with an increased AT when considering specific RVOT regions of BrS patients. Regardless of the technique used for signal acquisition and the methods of analysis, almost all epicardial studies identified a region in the RVOT epicardium of BrS patients harboring abnormally fractionated EGMs, whereas results in the

TABLE 3 Duration of bipolar electrograms from BrS patients in different clinical studies.

References (n° of patients)	Epicardial fractionation (ms)	Endocardial fractionation (ms)	Epicardial fractionation challenge (ms)	Endocardial fractionation challenge (ms)
Pappone et al. ⁷				
Symptomatic VF (39)	230[192-234]		330[310-333]	
Symptomatic no VF (24)	185[157-227]		310[280-330]	
Asymptomatic (72)	177[150-226]	-	300[260-330]	-
Nademanee et al. ³⁷				
Baseline, BCL 750 ms (32)	112 ± 48			
Baseline, 1:1 capture (32)	143 ± 66	-	-	-
Haïssaguerre et al. ⁴⁶				
BrS (6)	-	-	131 ± 34	-
Nademanee et al. ⁴⁹				
BrS anterior RV (9)	76 ± 28	66 ± 21		
BrS anterior RVOT (9)	132 ± 48	66 ± 21	-	-
Postema et al. ²⁷				
BrS type 1 (9)		83 ± 3		
BrS type 2 (10)		76 ± 2		
Control (9)	-	63 ± 2	-	-
Letsas et al. ⁴⁵				
BrS (10)	-	94.7 ± 21.2	-	-

Note: Results are as mean ± standard deviation or median and interquartile range. All studies performed electroanatomical mapping.

TABLE 4 Results from studies that performed CMR in BrS patients.

References	Cohort	cMR findings
Catalano et al. ⁵⁰	30 BrS versus 30 matched Hc	↓ RVOT EF n.s. RVOT area ↑ RV ESV ↑ RV inflow tract diameter
Papavassiliu et al. ^{51,52}	43 type 2/3 BrS versus 30 Hc	↓RV EF n.s. RVOT area n.s. RV ESV
Papavassiliu et al. ^{51,52}	26 Type 1 BrS versus 30 Hc	↓RV EF ↑ RVOT area ↑ RV ESV
Van Hoorn et al. ⁵³	138 BrS versus 18 Hc	↓RV EF ↑RVOT area ↑RV ESV LGE in 7/138 BrS
Tessa et al. ⁵⁴	29 BrS versus 29 Hc	n.s. RV EF n.s. RVOT area n.s. RV ESV LGE in 0/24 BrS
Rudic et al. ⁵⁵	81 BrS versus 30 Hc	↓RV EF ↑RVOT area ↑RV ESV LGE in 1/60 BrS
Bastiaenen et al. ⁵⁶	78 BrS versus 78 Hc	↓RV EF ↑RV ESV LGE in 6/78 BrS
Gray et al. ⁵⁷	29 BrS versus 29 Hc versus 17 ARVC	n.s. RVEF versus control, ↑ versus ARVC ↑RVOT volume versus control, n.s. versus ARVC No LGE in any group
Hohneck et al. ⁵⁸	106 BrS versus 25 Hc	↓RV EF ↑RVOT area ↑RV ESV LGE in 0/83 BrS
Pappone et al. ⁵⁹	24 BrS versus 24 Hc	n.s. RV EF ($p = .497$) n.s. RVOT area ($p = .156$) ↓ RV ESV No LGE in 24 patients
Pappone et al. ⁵⁹	24 BrS ajm versus 24 Hc ajm	↓ RV EF n.s. RV ESV
Isbister et al. ⁶⁰	18 BrS, longitudinal	↓RV EF in time ↑RV ESV in time 4/18 BrS developed LGE

Note: For all considered studies, the statistical significance when comparing two groups is established at $p = .05$, however, each study used different corrections for multiple comparisons.

Abbreviations: Hc, healthy controls; n.s., nonsignificant.

endocardial side are similar but are not obtained consistently between studies. This highlights the relation between AT, area with EGM fractionation, and type 1 ECG pattern.

3 | STRUCTURAL AND MORPHOLOGICAL ABNORMALITIES

The presence and role of structural abnormalities in BrS have long been debated. The findings in BrS patients concerning structural and morphological abnormalities are reported in Tables 4 and 5. In each study considered, there are additional findings that are not reported in the tables for the sake of clarity but are discussed separately in this paragraph. Almost every cardiac magnetic resonance (cMR) study on BrS patients found a trend toward a subclinical increase in RVOT area and reduction in RV ejection fraction (EF) (Table 4), while results from histologic studies report an increase in fibrosis content in the RV, especially in the RVOT (Table 5).

3.1 | Results from cMR studies

The presence of structural abnormalities in BrS has now been widely accepted since their initial discovery in postmortem histologic studies.²¹ The current matter of debate is the role of such morphological derangement in arrhythmogenesis and its evolution during the progression of the pathology. To date, despite several cMR studies on BrS patients, it is still debated whether structural abnormalities can be accurately detected with noninvasive techniques and whether they can have any implication in BrS diagnosis and prognosis. cMR studies in BrS patients focus on three categories of findings: morphological, functional, and contrast agent analysis (Late Gadolinium Enhancement, LGE)—which is considered the gold standard to assess myocardial fibrosis.^{66,67} There are differences between morphological and functional parameters when comparing BrS patients and control cohorts (Table 4). The results differ among studies, nonetheless, there is a trend toward reduced RV functional parameters and increased RV volumes when comparing BrS patients and healthy controls. RV morphological abnormalities were found in a high percentage of the studies considered in Table 4; here, we reported only data regarding RVOT area and RV end-systolic volume (ESV) since these parameters were evaluated in almost every study and are easily interpreted. In BrS patients, compared with controls, RVOT area was increased in 4 out of 8 studies, and RV ESV was increased in 7 out of 10 studies. In addition to morphological abnormalities, functional abnormalities were present in BrS patients. We reported results about RV EF, which was significantly lower in BrS patients in six out of nine studies (Table 4). Interestingly, studies correlated the presence of spontaneous type 1 ECG,⁵¹ or the presence of an SCN5A mutation^{53,59} with larger cardiac volumes and

TABLE 5 Results from histologic studies on BrS patients.

References	Cohort	Sampling location	Interstitial fibrosis	Fatty infiltration	Inflammatory infiltrates
Frustaci et al. ⁶¹	18 BrS phenotype	8–10 septal/apical LV/RV	–	–	14/18
Zumhagen et al. ⁶²	21 BrS	3–5 RVOT, septal RV	5/21	10/21	0/21
Ohkubo et al. ⁶³	25 BrS	1–3 upper septal RV	16/25 mild	10/25 mild	4/25 mild
Nademanee et al. ²¹	6 BrS	RV epicardium EAM guided	6/6	–	–
Nademanee et al. ²¹	6 p.m. BrS versus 6 p.m. Hc	Whole heart	Increased fibrosis percentage	n.s.	–
Pieroni et al. ⁶⁴	20 BrS	3–4 RVOT EAM guided	20/20 mild	0/20	12/20
Miles et al. ⁶⁵	28 p.m. BrS versus 29 p.m. Hc	Whole heart	Increased fibrosis percentage	n.s.	–

Abbreviations: Hc, healthy controls; n.s., nonsignificant; p.m., postmortem cohort.

lower EF. The role of sodium current is further underlined by the study of Pappone et al.,⁵⁹ who did not find a significant difference in EF between BrS patients and controls at baseline, however after ajmaline challenge the reduction in EF became significant. LGE seems to be a very rare finding in BrS cohorts: only three of seven studies found evidence of LGE in a small percentage of their BrS cohort, and it was almost always located in the interventricular septum. The lack of consistency in LGE results is probably due both to the thinness of the RV wall and to the apparent development of structural abnormalities in time.⁶⁰ Fibrosis was consistently found in postmortem studies.^{21,65} However, such anatomical disarray may not represent the majority of BrS patients, most of whom remain asymptomatic and do not present fibrosis at the noninvasive evaluation.^{56,60} Indeed, in the studies considered, LGE was never found in more than 10% of patients examined; when present, it was often localized in the interventricular septum, whereas the region with the highest amount of fibrosis in histologic postmortem studies was the RVOT. Thus it is likely that LGE MRI is not sensitive enough to detect diffuse fibrosis in the RVOT. Finally, the inconsistency of LGE findings can be partly imputed to the fact that usually symptomatic BrS patients have an ICD and can not undergo a standard LGE examination.⁵⁷ In conclusion, cMR can reveal morphological and functional abnormalities in BrS patients, which point toward RV dysfunction. However, as reported in several studies,⁵⁵ these structural abnormalities are mostly subclinical. Currently, it is not known if the reduction in RV functionality plays any role in BrS, nor if it is determined by electrophysiological modifications and/or by a genetic background.

3.2 | Results from histological studies

Increased fibrosis is a consistent finding both in whole heart histology and in vivo biopsy in BrS patients. Nademanee et al.²¹ were the first to identify increased collagen and reduced expression of connexin-43 in five postmortem BrS hearts compared with six controls. Such

observations were further sustained by the presence of fibrosis when performing in vivo epicardial biopsy in areas with fractionated EGMs of six BrS patients.²¹ Miles et al.⁶⁵ confirmed the increase in collagen content in a postmortem cohort of BrS patients compared with controls. Furthermore, inflammatory infiltrates were found in the heart of BrS patients,^{61,63,64} but the significance of such a finding is still controversial. In Table 5 we summarized the main findings of each histologic study on BrS patients examined in this work. Each study provided additional findings which are not reported for the sake of clarity. Most patients enrolled in the studies of Table 5 presented subtle structural abnormalities that were not detected by routine examinations (cMR, postmortem examination, or echocardiographic imaging). Postmortem studies have identified an increase in collagen deposition through the whole heart of BrS patients when compared with controls, with the maximum difference in the RVOT epicardium. Nademanee et al.²¹ found an average increase from 10.5% to 13.9% in collagen content in the epicardial RVOT, while Miles et al.⁶⁵ found an increase from 15.4% to 23.7%. As previously discussed, noninvasive imaging has not been able to effectively detect fibrosis in BrS hearts, whereas EAM seems more sensitive: both Pieroni et al.⁶⁴ and Nademanee et al.^{21,37} have demonstrated that areas with low voltage and fractionated/late EGMs harbor structural abnormalities. Different results between studies may be imputed to different sampling locations (e.g., EAM-guided or random), quantification procedures (qualitative vs. quantitative), and the presence of controls as a reference in qualitative assessment. To date, the presence of inflammatory and fatty infiltrates in BrS patients is still debated.^{64,68,69} Frustaci et al.⁶¹ were the first to report a significant presence of inflammatory infiltrates in the cardiac tissue of patients with clinical phenotype of BrS (type 1 ECG and arrhythmic history or familial arrhythmic history); however, this study included several patients with myocarditis (in which the BrS pattern disappeared during follow-up). In the following years, the presence of inflammatory infiltrates was found by two studies,^{64,70} but these observations were not further confirmed by other studies (refer to Table 5). Pieroni et al.⁶⁴ proposed that fibrotic deposition in the RVOT of a BrS heart

could be due to temporary myocardial inflammation and subsequent connexin-43 downregulation.^{66,67,71} Several studies reported the presence of myocardial inflammation in BrS, however, its role needs to be elucidated.⁷² Furthermore, studies demonstrated that patients with cardiac structural abnormalities can exhibit a Brugada ECG phenotype and clinical features.^{61,73} Of note, recent studies have drawn attention to the possible electrophysiological implications of inflammation in the myocardial tissue and evidenced overlapping features of BrS and arrhythmogenic cardiomyopathy (ACM), where the presence of fibro-fatty infiltration is consolidated.^{74–76} In conclusion, an increase in fibrosis content is a frequently described substrate alteration in the RVOT of BrS patients. The presence and possible role of myocardial inflammation in BrS pathogenesis and progression still needs investigation.

4 | DISCUSSION

4.1 | Current limitations

To date, data regarding the electrophysiological and anatomical substrate of BrS are abundant but sometimes contradicting. First, AP abnormalities are difficult to assess *in vivo*. Furthermore, clinical studies found conflicting results comparing APD of patients and controls, it follows that hypotheses concerning APD are difficult to assess. On the contrary, delayed depolarization and conduction block in the RVOT epicardial layer at high-frequency pacing is a robust finding, further supported by the presence of EGM fractionation in the same substrate, which is related to delayed activation. Likewise, the abnormal amount of diffuse fibrosis in the RVOT is also a recurrent finding, as well as slightly abnormal right ventricular morphological and functional parameters evaluated at cMR. Even though the presence of both electrical and anatomical abnormalities in BrS has been described in clinical and experimental studies, the interplay between them and their role in the manifestation of the BrS phenotype and arrhythmogenesis is not clear. The main hypotheses on the BrS phenotype and arrhythmogenesis tend to consider only one aspect of the BrS substrate, either structural (depolarization hypothesis) or electrophysiological (repolarization hypothesis). In recent years, new theories tried to explain the genesis of the BrS phenotype, however, their validation is limited by the relatively low number of arrhythmic events in BrS patients (which lowers statistical significance), and the limitations of animal models in a setting where both the causes of the pathology and the translational value are debated.⁷⁷ In this context, mathematical computational models have demonstrated their usefulness in simulating realistic scenarios to study pathogenesis and to develop risk stratification strategies. Today, computational models can reproduce the normal electrophysiological activity of the heart embedded in a detailed anatomical geometry (from ventricles to atria, to the torso,...), with a realistic physiological activation pattern and ECG generation.⁷⁸ The reliability of the results of computational models is founded on solid data to validate the approach, while the interpretation of nonquantitative

clinical findings as parameters in a computational model is difficult or arbitrary.⁷⁹ As shown in the previous sections, there are few solid quantitative findings on BrS patients, creating an obstacle to the development of mathematical computational models for this pathology.

4.2 | Role of structural and electrophysiological abnormalities

In a recent attempt to include both electrophysiological and structural parameters, Boukens et al.^{80,81} proposed that the human RVOT maintains part of its embryonic phenotype, which results in conduction slowing and electrophysiological heterogeneity that become manifest when sodium current is reduced. Indeed, the human RV contains more fat and collagen than the LV,⁸² and studies on animals have shown that the RV has more structural discontinuities^{83,84} and reduced expression of sodium currents⁸⁵ when compared with LV. To illustrate a simplified computational integration to the hypothesis of Boukens et al.,^{80,81} we performed a proof-of-concept numerical simulation to show depolarization in the presence of structural discontinuity, depolarization current reduction, and the combination of both (Figure 2). The myocyte model used in the simulation was previously developed by our group,^{86,87} diffuse fibrosis was modeled as randomly scattered unexcitable obstacles in the computational domain.⁸⁸ Depolarization in the presence of structural abnormalities when sodium current is preserved results in delayed depolarization without significant abnormalities in the activation pattern, as outlined in Figure 2A. A similar behavior is shown in Figure 2C, where the reduction in sodium current without structural abnormalities does not change significantly the depolarization pattern, resulting in homogeneous delayed depolarization. When both impairment of sodium current and structural abnormalities are present (Figure 2B), depolarization is significantly affected inducing a delayed activation in an explanation-relevant amount of tissue. In brief, Boukens et al.⁸⁰ hypothesized that the proarrhythmic substrate is created when structural and electrophysiological abnormalities coexist.⁸⁹ In support of this hypothesis, Hoogendijk et al.⁹⁰ provided further evidence of the role of sodium current in the robustness of propagation, by showing that conduction through inexcitable isthmuses is blocked when sodium current is reduced in pig heart wedges. As proposed by Behr et al.⁹¹ and illustrated in Figure 2, reduction in sodium current has more effect on regions with a higher degree of structural abnormalities. In the setting of BrS, the structural abnormalities are mostly “static,” and generally present an increasing gradient from RVA to RVOT, from endocardium to epicardium.^{21,65} The interplay between electrophysiological and structural abnormalities also holds in the presence of repolarization abnormalities in the tissue. By using computational models, it has been shown that the presence of diffuse fibrosis creates reentrant circuits when short APs are present,⁹² a mechanism known as “reentry by percolation.” In particular, reentry occurs when the excitation wave anchors on an obstacle with a suitable dimension.

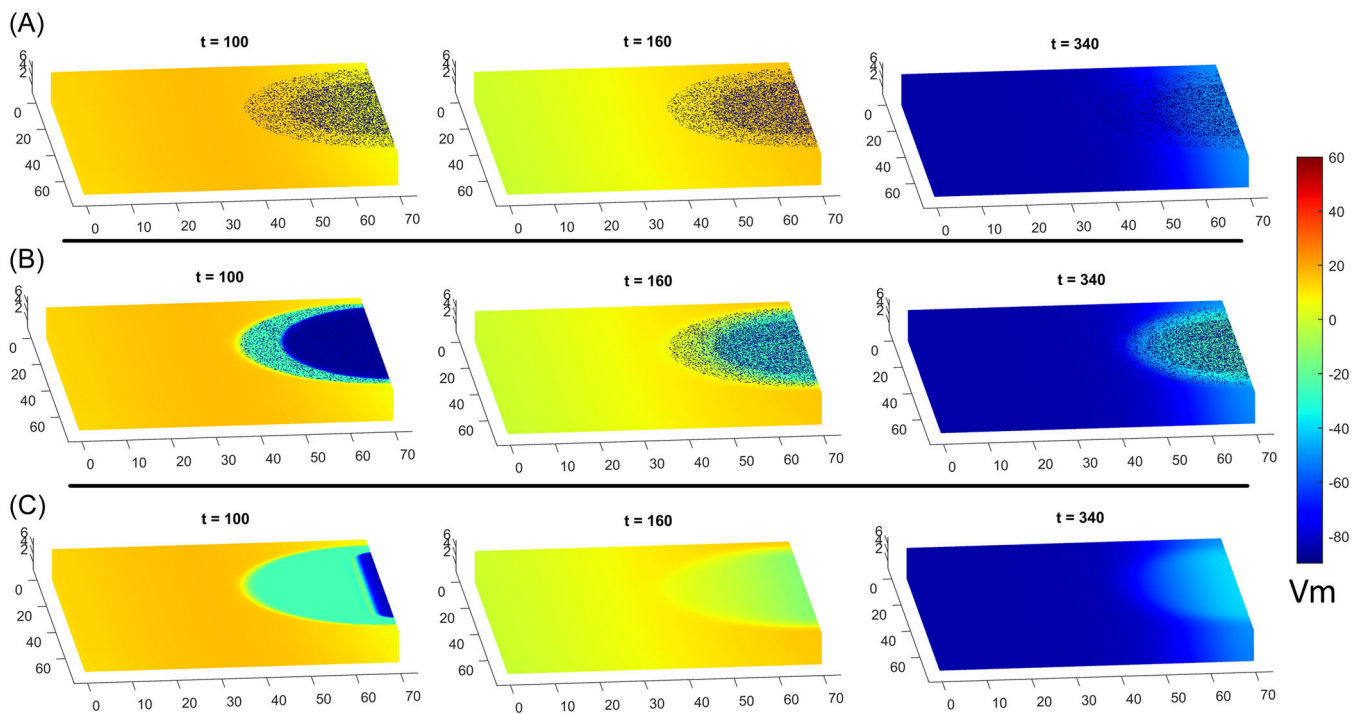


FIGURE 2 Illustration depicting the membrane potential (V_m) during a depolarization sequence in a $7 \times 7 \times 0.7$ cm slab of cardiac tissue, time in milliseconds. The slab is composed of healthy myocardium with a semicircular substrate on the right, each row shows a different alteration in the substrate. (A) substrate with structural abnormalities in electrical healthy tissue. (B) substrate with structural abnormalities and reduced sodium current. (C) substrate with reduced sodium current.

Alonso et al.⁹² showed that the risk of reentry is modulated by the density of unexcitable obstacles in the cardiac tissue and the wavelength of cardiac excitation (expressed as $APD \times$ conduction velocity). In brief, the shorter the wavelength the fewer obstacles are needed to cause reentry. Likewise, Szél et al.¹⁸ showed that an extreme reduction in APD (i.e., lost dome AP) is enough to generate arrhythmic behavior in a wedge of canine heart. We can consider this as the limit case of the computational example⁹² where the APD is so low that minimal obstacles are enough to cause reentry. In this context, any electrophysiological abnormality that shortens the APD modulates the risk of reentry along with the density of structural abnormality present in the heart of BrS patients. Data from patients' findings seem to support both hypotheses: Pappone et al.⁷ noted that EGMs fractionation increases when moving toward the center of the BrS substrate (the zone with the highest degree of structural abnormality); the group also documented an enlargement of the pathologically fractionated area after ajmaline administration.

4.3 | Translational outlook

All these experimental observations and hypotheses, however, cannot be used to decide if a patient is at immediate risk of arrhythmia, or to understand how the arrhythmic trigger and sustaining occurs. As an example, we know that the degree of ST elevation in the type 1 ECG is related to the area of abnormal

electrophysiological substrate, however, it is not possible to establish how, or how much abnormality or substrate area are needed to generate a surface signal, or how the substrate area affects arrhythmogenesis. In this direction, a recent computational study⁹³ has explored the effect of conduction slowing and early repolarization on the surface ECG, confirming that the presence of the ECG pattern is related to the abnormal substrate in the epicardial RVOT. As noted in several studies,⁸⁹ EGMs fractionation in the BrS substrate is present regardless of a surface type 1 ECG. It is plausible that EGMs fractionation is caused by a moderate degree of structural and electrophysiological abnormality which results in conduction delay, whereas type 1 ECG is manifested only when a critical threshold in depolarization impairment is reached. Using a computational setup to simulate the RV, all the variables described in previous observational studies (such as slow conducting regions, fibrosis, different ionic mutations, positions of the substrate,...) can be included to understand the effect of the BrS substrate on the surface ECG.^{70,94,95} Furthermore, since many patients do not have a permanent type 1 pattern,^{96–98} the modeling approach could help define how physiological variables (e.g., sodium current availability) modulate the presence and position of ST elevation in the ECG. The main drawback of this approach is that the various features modeled must be validated in cohorts of patients. Nonetheless, computational models can be used as a physics-based and explainable insight to choose which risk markers are related to the BrS substrate.

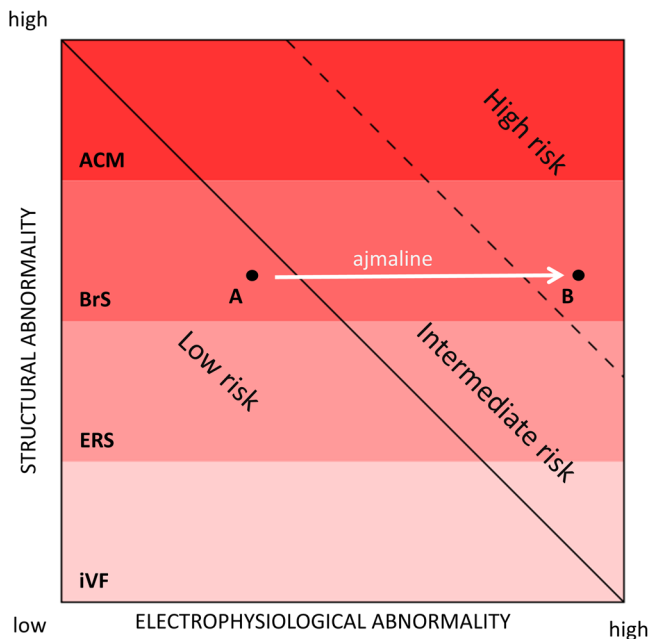


FIGURE 3 Example of a risk plane in BrS patients: the arrhythmic risk is a combination of structural (y axis) and electrophysiological (x axis) abnormalities that can be increased by modulating factors like acute sodium reduction from ajmaline. ACM, arrhythmogenic cardiomyopathy; BrS, Brugada syndrome; ERS, early repolarization syndrome; iVF, idiopathic ventricular fibrillation. Adapted from Weiss,¹⁰⁰ Boukens et al.,¹⁰¹ Hoogendijk et al.¹⁰²

4.4 | Definition of the arrhythmic risk

Recently, Miles et al.⁹⁹ proposed that BrS, early repolarization syndrome (ERS), and idiopathic ventricular fibrillation (iVF) are based on similar pathologic basis but are distinguished by the extent of structural abnormalities in the cardiac substrate. iVF abnormalities are detectable only in histology, ERS abnormalities are detected by EAM, BrS abnormalities are sometimes detectable even with noninvasive techniques. As proposed by Weiss,¹⁰⁰ a similar spectrum of abnormality might exist in electrophysiological alteration (from subtle alterations to manifest activation/repolarization abnormalities), so that both structural and electrophysiological abnormalities concur to define the patient's arrhythmic risk (see Figure 3). The classification of cardiac pathologies according to the detectability of structural abnormality divides the risk plane into four regions, each corresponding to a different pathology⁹⁹; we add the level of electrophysiological impairment to affect the arrhythmic risk further. Consider a BrS patient with a low level of electrophysiological imbalance (point A in Figure 3). At baseline, the patient is at low arrhythmic risk since the level of structural derangement alone is not sufficient to precipitate VF. However, when a sudden increase in electrophysiological abnormality occurs (e.g., reduction in sodium current after ajmaline administration), the patient moves to another point in the risk plane since its level of electrophysiological imbalance has increased (point B in Figure 3), now resulting in a high arrhythmic

risk. In a previous computational work of our group regarding BrS, we related structural and electrophysiological abnormalities to a possible mechanism of arrhythmia in a computational model of BrS.^{87,103} We observed that the likelihood of arrhythmia was a function of the structural alteration and electrophysiological alteration and demonstrated that the plane defined by these two parameters defines regions of low and high probability of arrhythmia. The application of this model to clinical risk stratification context requires the identification of which physiological quantities are related to the modeled structural and electrophysiological alterations (e.g., EGM fractionation as a marker of structural alteration), and how their values are related to the values modeled in the computational setup. In conclusion, we believe that in addition to a spectrum of structural abnormalities, electrophysiological derangement can be thought of as a spectrum and, in combination with structural alterations, modulates arrhythmic risk. This interpretation of structural and electrophysiological derangement could help in the interpretation of conditions where apparently no structural abnormality is detected, but strong sodium reduction is present.¹⁰⁴ Even though experimental data seem to point in this direction, to date there is no validation of this hypothesis and further clarification is needed. In this context, computational studies allow a wide range of explorative setups and could help define arrhythmic risk algorithms to be tested in specific clinical contexts.

5 | CONCLUSION

Despite recent advances in the definition of the BrS substrate, a lot of open questions remain. The arrhythmogenic mechanism of BrS remains unknown and none of the currently proposed hypotheses have been fully confirmed in an *in vivo* setting. Although data on anatomical and electrical abnormalities in the BrS substrate are scattered and sometimes contradicting, we were able to summarize and report consistent pathological findings present in the literature. Epicardial activation delay and conduction block characterize the RVOT of BrS patients and are likely related to the ECG phenotype and arrhythmogenic mechanism; evidence suggests that the latter is caused by the interplay between anatomical and electrophysiological abnormalities.^{99,100,105} An innovative approach that might shed light on the role of structural abnormalities in BrS might be to consider BrS and other related pathologies as a spectrum of a "common pathway" of electrophysiological and structural substrates, rather than strictly defined categories. In this context, computational models are an emerging tool that can support the understanding of the BrS phenotype and improve risk stratification strategies.

DATA AVAILABILITY STATEMENT

Data sharing is not applicable to this article as no new data were created or analyzed in this study.

ORCID

Niccolò Biasi  <http://orcid.org/0000-0001-8194-1010>

REFERENCES

- Letsas KP, Asvestas D, Baranchuk A, et al. Prognosis, risk stratification, and management of asymptomatic individuals with Brugada syndrome: a systematic review. *Pacing Clin Electrophysiol*. 2017;40(12):1332-1345. doi:10.1111/pace.13214
- Priori SG, Gasparini M, Napolitano C, et al. Risk stratification in Brugada syndrome. *J Am Coll Cardiol*. 2012;59(1):37-45. doi:10.1016/j.jacc.2011.08.064
- Probst V, Veltmann C, Eckardt L, et al. Long-term prognosis of patients diagnosed with Brugada syndrome. *Circulation*. 2010;121(5):635-643. doi:10.1161/CIRCULATIONAHA.109.887026
- Milman A, Andorin A, Gourraud J-B, et al. Age of first arrhythmic event in Brugada syndrome: data from the SABRUS (Survey on Arrhythmic Events in Brugada Syndrome) in 678 patients. *Circ Arrhythm Electrophysiol*. 2017;10(12):e005222. doi:10.1161/CIRCEP.117.005222
- Zeppenfeld K, Tfelt-Hansen J, De Riva M, et al. 2022 ESC Guidelines for the management of patients with ventricular arrhythmias and the prevention of sudden cardiac death. *Eur Heart J*. 2022;43(40):3997-4126. doi:10.1093/eurheartj/ehac262
- Zhang P, Tung R, Zhang Z, et al. Characterization of the epicardial substrate for catheter ablation of Brugada syndrome. *Heart Rhythm*. 2016;13(11):2151-2158. doi:10.1016/j.hrthm.2016.07.025
- Pappone C, Brugada J, Vicedomini G, et al. Electrical Substrate Elimination in 135 Consecutive Patients With Brugada Syndrome. *Circ Arrhythm Electrophysiol*. 2017;10(5):e005053. doi:10.1161/CIRCEP.117.005053
- Pappone C, Mecarocci V, Manguso F, et al. New electromechanical substrate abnormalities in high-risk patients with Brugada syndrome. *Heart Rhythm*. 2020;17(4):637-645. doi:10.1016/j.hrthm.2019.11.019
- Nademanee K, Chung F-P, Sacher F, et al. Long-term outcomes of Brugada substrate ablation: a report from BRAVO (Brugada Ablation of VF Substrate Ongoing Multicenter Registry). *Circulation*. 2023;147(21):1568-1578. doi:10.1161/CIRCULATIONAHA.122.063367
- Chung CT, Bazoukis G, Radford D, et al. Predictive risk models for forecasting arrhythmic outcomes in Brugada syndrome: a focused review. *J Electrocardiol*. 2022;72:28-34. doi:10.1016/j.jelectrocard.2022.02.009
- Shinohara T, Takagi M, Kamakura T, et al. Long-term prognosis in patients with non-type 1 Brugada electrocardiogram: results from a large Japanese cohort of idiopathic ventricular fibrillation. *Ann Noninvasive Electrocardiol*. 2021;26(4):e12831. doi:10.1111/anec.12831
- Lee S, Zhou J, Chung CT, et al. Comparing the performance of published risk scores in Brugada syndrome: a multi-center cohort study. *Curr Probl Cardiol*. 2022;47(12):101381. doi:10.1016/j.cpcardiol.2022.10138
- Shinohara T, Takagi M, Kamakura T, et al. Risk stratification in asymptomatic patients with Brugada syndrome: utility of multiple risk factor combination rather than programmed electrical stimulation. *J Cardiovasc Electrophysiol*. 2021;32(2):507-514. doi:10.1111/jce.14848
- Takagi M, Sekiguchi Y, Yokoyama Y, et al. The prognostic impact of single extra-stimulus on programmed ventricular stimulation in Brugada patients without previous cardiac arrest: multi-centre study in Japan. *EP Eur*. 2018;20(7):1194-1200. doi:10.1093/europace/eux096.16
- Gaita F, Cerrato N, Giustetto C, et al. Asymptomatic patients with Brugada ECG pattern: long-term prognosis from a large prospective study. *Circulation*. 2023;148(20):1543-1555. doi:10.1161/CIRCULATIONAHA.123.064689
- Asada S, Morita H, Watanabe A, et al. Indication and prognostic significance of programmed ventricular stimulation in asymptomatic patients with Brugada syndrome. *EP Eur*. 2020;22(6):972-979. doi:10.1093/europace/ea003
- Sroubek J, Probst V, Mazzanti A, et al. Programmed ventricular stimulation for risk stratification in the Brugada syndrome. *Circulation*. 2016;133(7):622-630. doi:10.1161/CIRCULATIONAHA.115.017885
- Szél T, Antzelevitch C. Abnormal repolarization as the basis for late potentials and fractionated electrograms recorded from epicardium in experimental models of Brugada syndrome. *J Am Coll Cardiol*. 2014;63(19):2037-2045. doi:10.1016/j.jacc.2014.01.067
- Antzelevitch C. Transmural dispersion of repolarization and the T wave. *Cardiovasc Res*. 2001;50(3):426-431. doi:10.1016/S0008-6363(01)00285-1
- Yan G-X, Antzelevitch C. Cellular basis for the Brugada syndrome and other mechanisms of arrhythmogenesis associated with ST-segment elevation. *Circulation*. 1999;100(15):1660-1666. doi:10.1161/01.CIR.100.15.1660
- Nademanee K, Raju H, de Noronha SV, et al. Fibrosis, connexin-43, and conduction abnormalities in the Brugada syndrome. *J Am Coll Cardiol*. 2015;66(18):1976-1986. doi:10.1016/j.jacc.2015.08.862
- Ino T, Karagueuzian HS, Hong K, Meesmann M, Mandel WJ, Peter T. Relation of monophasic action potential recorded with contact electrode to underlying transmembrane action potential properties in isolated cardiac tissues: a systematic microelectrode validation study. *Cardiovasc Res*. 1988;22(4):255-264. doi:10.1093/cvr/22.4.255
- Irvanian S, Uzelac I, Herndon C, Langberg JJ, Fenton FH. Generation of monophasic action potentials and intermediate forms. *Biophys J*. 2020;119(2):460-469. doi:10.1016/j.bpj.2020.05.039
- Potse M, Vinet A, Opthof T, Coronel R. Validation of a simple model for the morphology of the T wave in unipolar electrograms. *Am J Physiol Heart Circ Physiol*. 2009;297(2):H792-H801. doi:10.1152/ajpheart.00064.2009
- Western D, Hanson B, Taggart P. Measurement bias in activation-recovery intervals from unipolar electrograms. *Am J Physiol Heart Circ Physiol*. 2015;308(4):H331-H338. doi:10.1152/ajpheart.00478.2014
- Coronel R, de Bakker JMT, Wilms-Schopman FJG, et al. Monophasic action potentials and activation recovery intervals as measures of ventricular action potential duration: experimental evidence to resolve some controversies. *Heart Rhythm*. 2006;3(9):1043-1050. doi:10.1016/j.hrthm.2006.05.027
- Postema PG, van Dessel PF, de Bakker JM, et al. Slow and discontinuous conduction conspire in Brugada syndrome. *Circ Arrhythm Electrophysiol*. 2008;1(5):379-386. doi:10.1161/CIRCEP.108.790543
- Nagase S, Kusano KF, Morita H, et al. Longer repolarization in the epicardium at the right ventricular outflow tract causes type 1 electrocardiogram in patients with Brugada syndrome. *J Am Coll Cardiol*. 2008;51(12):1154-1161. doi:10.1016/j.jacc.2007.10.059.17
- Zhang J, Sacher F, Hoffmayer K, et al. Cardiac electrophysiological substrate underlying the ECG phenotype and electrogram abnormalities in Brugada syndrome patients. *Circulation*. 2015;131(22):1950-1959. doi:10.1161/CIRCULATIONAHA.114.013698
- Galli A, Rizzo A, Monaco C, et al. Electrocardiographic imaging of the arrhythmogenic substrate of Brugada syndrome: current evidence and future perspectives. *Trends Cardiovasc Med*. 2021;31(5):323-329. doi:10.1016/j.tcm.2020.06.004
- Ashino S, Watanabe I, Kofune M, et al. Abnormal action potential duration restitution property in the right ventricular outflow tract in Brugada syndrome. *Circ J*. 2010;74(4):664-670. doi:10.1253/circj.CJ-09-0872

32. Ashino S, Watanabe I, Kofune M, et al. Effects of quinidine on the action potential duration restitution property in the right ventricular outflow tract in patients with brugada syndrome. *Circ J*. 2011;75(9):2080-2086. doi:10.1253/circj.CJ-11-0227
33. Nishii N, Nagase S, Morita H, et al. Abnormal restitution property of action potential duration and conduction delay in Brugada syndrome: both repolarization and depolarization abnormalities. *Europace*. 2010;12(4):544-552. doi:10.1093/europace/eup432
34. Hayashi M, Takatsuki S, Maison-Blanche P, et al. Ventricular repolarization restitution properties in patients exhibiting type 1 Brugada electrocardiogram with and without inducible ventricular fibrillation. *J Am Coll Cardiol*. 2008;51(12):1162-1168. doi:10.1016/j.jacc.2007.11.050
35. Rudic B, Chaykovskaya M, Tsyganov A, et al. Simultaneous non-invasive epicardial and endocardial mapping in patients with Brugada syndrome: new insights into arrhythmia mechanisms. *J Am Heart Assoc*. 2016;5(11):e004095. doi:10.1161/JAHA.116.004095
36. Pannone L, Monaco C, Sorgente A, et al. Ajmaline-induced abnormalities in Brugada syndrome: evaluation with ECG imaging. *J Am Heart Assoc*. 2022;11(2):e024001. doi:10.1161/JAHA.121.024001
37. Nademanee K, Veerakul G, Nogami A, et al. Mechanism of the effects of sodium channel blockade on the arrhythmogenic substrate of Brugada syndrome. *Heart Rhythm*. 2022;19(3):407-416. doi:10.1016/j.hrthm.2021.10.031
38. Langfield P, Feng Y, Bear LR, et al. A novel method to correct repolarization time estimation from unipolar electrograms distorted by standard filtering. *Med Image Anal*. 2021;72:102075. doi:10.1016/j.media.2021.102075
39. Rossi A, Giannoni A, Nesti M, et al. Prognostic value of right ventricular refractory period heterogeneity in Type-1 Brugada electrocardiographic pattern. *EP Eur*. 2023;25(2):651-659. doi:10.1093/europace/euac168
40. Renard E, Walton RD, Benoist D, et al. Functional epicardial conduction disturbances due to a SCN5A variant associated with Brugada syndrome. *JACC Clin Electrophysiol*. 2023;9(8_Part_1):1248-1261. doi:10.1016/j.jacep.2023.03.009
41. Zhong R, Schimanski T, Zhang F, et al. A preclinical study on Brugada syndrome with a CACNB2 variant using human cardiomyocytes from induced pluripotent stem cells. *Int J Mol Sci*. 2022;23(15):8313. doi:10.3390/ijms23158313
42. Kurita T, Shimizu W, Inagaki M, et al. The electrophysiologic mechanism of ST-segment elevation in Brugada syndrome. *J Am Coll Cardiol*. 2002;40(2):330-334. doi:10.1016/S0735-1097(02)01964-2
43. Aras K, Gams A, Faye NR, et al. Electrophysiology and arrhythmogenesis in the human right ventricular outflow tract. *Circ Arrhythm Electrophysiol*. 2022;15(3):e010630. doi:10.1161/CIRCEP.121.010630.18
44. Lambiase PD, Ahmed AK, Ciaccio EJ, et al. High-density substrate mapping in Brugada syndrome: combined role of conduction and repolarization heterogeneities in arrhythmogenesis. *Circulation*. 2009;120(2):106-117. doi:10.1161/CIRCULATIONAHA.108.771401
45. Letsas KP, Efremidis M, Vlachos K, et al. Right ventricular outflow tract high-density endocardial unipolar voltage mapping in patients with Brugada syndrome: evidence for electroanatomical abnormalities. *EP Eur*. 2018;20(F11):f57-f63. doi:10.1093/europace/eux079
46. Haïssaguerre M, Nademanee K, Sacher F, et al. Multisite conduction block in the epicardial substrate of Brugada syndrome. *Heart Rhythm*. 2022;19(3):417-426. doi:10.1016/j.hrthm.2021.10.030
47. Haïssaguerre M, Cheniti G, Nademanee K, et al. Dependence of epicardial T-wave on local activation voltage in Brugada syndrome. *Heart Rhythm*. 2022;19(10):1686-1688. doi:10.1016/j.hrthm.2022.05.036
48. Letsas KP, Vlachos K, Conte G, et al. Right ventricular outflow tract electroanatomical abnormalities in asymptomatic and high-risk symptomatic patients with Brugada syndrome: evidence for a new risk stratification tool? *J Cardiovasc Electrophysiol*. 2021;32(11):2997-3007. doi:10.1111/jce.15262
49. Nademanee K, Veerakul G, Chandanamatta P, et al. Prevention of ventricular fibrillation episodes in Brugada syndrome by catheter ablation over the anterior right ventricular outflow tract epicardium. *Circulation*. 2011;123(12):1270-1279. doi:10.1161/CIRCULATIONAHA.110.972612
50. Catalano O, Antonaci S, Moro G, et al. Magnetic resonance investigations in Brugada syndrome reveal unexpectedly high rate of structural abnormalities. *Eur Heart J*. 2009;30(18):2241-2248. doi:10.1093/eurheartj/ehp252
51. Papavassiliu T, Veltmann C, Doesch C, et al. Spontaneous type 1 electrocardiographic pattern is associated with cardiovascular magnetic resonance imaging changes in Brugada syndrome. *Heart Rhythm*. 2010;7(12):1790-1796. doi:10.1016/j.hrthm.2010.09.004
52. Papavassiliu T, Wolpert C, Flüchter S, et al. MAGNETIC RESONANCE IMAGING FINDINGS IN PATIENTS WITH BRUGADA SYNDROME. *J Cardiovasc Electrophysiol*. 2004;15(10):1133-1138. doi:10.1046/j.1540-8167.2004.03681.x
53. van Hoom F, Campian ME, Spijkerboer A, et al. SCN5A mutations in Brugada syndrome are associated with increased cardiac dimensions and reduced contractility. *PLoS One*. 2012;7(8):e42037. doi:10.1371/journal.pone.0042037
54. Tessa C, Del Meglio J, Ghidini Ottonelli A, et al. Evaluation of Brugada syndrome by cardiac magnetic resonance. *Int J Cardiovasc Imaging*. 2012;28(8):1961-1970. doi:10.1007/s10554-012-0009-5
55. Rudic B, Schimpf R, Veltmann C, et al. Brugada syndrome: clinical presentation and genotype—correlation with magnetic resonance imaging parameters. *Europace*. 2016;18(9):1411-1419. doi:10.1093/europace/euv300
56. Bastiaenen R, Cox AT, Castelletti S, et al. Late gadolinium enhancement in Brugada syndrome: a marker for subtle underlying cardiomyopathy? *Heart Rhythm*. 2017;14(4):583-589. doi:10.1016/j.hrthm.2016.12.004
57. Gray B, Gnanappa GK, Bagnall RD, et al. Relations between right ventricular morphology and clinical, electrical and genetic parameters in Brugada Syndrome. *PLoS One*. 2018;13(4):e0195594. doi:10.1371/journal.pone.0195594.19
58. Hohneck A, Overhoff D, Rutsch M, et al. Risk stratification of patients with Brugada syndrome: the impact of myocardial strain analysis using cardiac magnetic resonance feature tracking. *Hell J Cardiol*. 2021;62(5):329-338. doi:10.1016/j.hjc.2021.05.003
59. Pappone C, Santinelli V, Mecarocci V, et al. Brugada syndrome: new insights from cardiac magnetic resonance and electroanatomical imaging. *Circ Arrhythm Electrophysiol*. 2021;14(11):e010004. doi:10.1161/CIRCEP.121.010004
60. Isbister JC, Gray B, Offen S, et al. Longitudinal assessment of structural phenotype in Brugada syndrome using cardiac magnetic resonance imaging. *Heart Rhythm O2*. 2023;4(1):34-41. doi:10.1016/j.hroo.2022.10.004
61. Frustaci A, Priori SG, Pieroni M, et al. Cardiac histological substrate in patients with clinical phenotype of Brugada syndrome. *Circulation*. 2005;112(24):3680-3687. doi:10.1161/CIRCULATIONAHA.105.520999
62. Zumhagen S, Spieker T, Rolinck J, et al. Absence of pathognomonic or inflammatory patterns in cardiac biopsies from patients with Brugada syndrome. *Circ Arrhythm Electrophysiol*. 2009;2(1):16-23. doi:10.1161/CIRCEP.107.737882
63. Ohkubo K, Watanabe I, Okumura Y, et al. Right ventricular histological substrate and conduction delay in patients with

- Brugada syndrome. *Int Heart J*. 2010;51(1):17-23. doi:10.1536/ihj.51.17
64. Pieroni M, Notarstefano P, Oliva A, et al. Electroanatomic and pathologic right ventricular outflow tract abnormalities in patients with Brugada syndrome. *J Am Coll Cardiol*. 2018;72(22):2747-2757. doi:10.1016/j.jacc.2018.09.037.
 65. Miles C, Asimaki A, Ster IC, et al. Biventricular Myocardial Fibrosis/myocardial fibrosis and Sudden Deaths/sudden death in Patients With Brugada Syndrome. *J Am Coll Cardiol*. 2021;78(15):1511-1521. doi:10.1016/j.jacc.2021.08.010
 66. Nguyen M-N, Kiriazis H, Gao X-M, Du X-J. Cardiac fibrosis and arrhythmogenesis. *Compr Physiol*. 2017;7:1009-1049. doi:10.1002/cphy.c160046
 67. López B, Ravassa S, Moreno MU, et al. Diffuse myocardial fibrosis: mechanisms, diagnosis and therapeutic approaches. *Nat Rev Cardiol*. 2021;18(7):479-498. doi:10.1038/s41569-020-00504-1
 68. Miles C, Asimaki A, Behr ER, Sheppard MN. Myocardial inflammation in Brugada syndrome. *J Am Coll Cardiol*. 2019;73(11):1369-1370. doi:10.1016/j.jacc.2018.12.058
 69. Frustaci A, Russo MA, Chimenti C. Structural myocardial abnormalities in asymptomatic family members with brugada syndrome and SCN5a gene mutation. *Eur Heart J*. 2009;30(14):11763. doi:10.1093/eurheartj/ehp148
 70. Coronel R, Casini S, Koopmann TT, et al. Right ventricular fibrosis and conduction delay in a patient with clinical signs of Brugada syndrome: a combined electrophysiological, genetic, histopathologic, and computational study. *Circulation*. 2005;112(18):2769-2777. doi:10.1161/CIRCULATIONAHA.105.532614
 71. Humeres C, Frangogiannis NG. Fibroblasts in the infarcted, remodeling, and failing heart. *JACC Basic Trans Sci*. 2019;4(3):449-467. doi:10.1016/j.jaccbts.2019.02.006
 72. Corrado D, Migliore F, Zorzi A. Brugada syndrome. *J Am Coll Cardiol*. 2018;72(22):2758-2760. doi:10.1016/j.jacc.2018.08.2199.20
 73. Corrado D, Basso C, Buja G, Nava A, Rossi L, Thiene G. Right bundle branch block, right precordial ST-segment elevation, and sudden death in young people. *Circulation*. 2001;103(5):710-717. doi:10.1161/01.cir.103.5.710
 74. Ben-Haim Y, Asimaki A, Behr ER. Brugada syndrome and arrhythmogenic cardiomyopathy: overlapping disorders of the connexome? *EP Europ*. 2021;23(5):653-664. doi:10.1093/europace/eaab277
 75. Corrado D, Zorzi A, Cerrone M, et al. Relationship between arrhythmogenic right ventricular cardiomyopathy and Brugada syndrome: new insights from molecular biology and clinical implications. *Circ Arrhythm Electrophysiol*. 2016;9(4):e003631. doi:10.1161/CIRCEP.115.003631
 76. Scheirlyncx E, Chivulescu M, Lie ØH, et al. Worse prognosis in Brugada syndrome patients with arrhythmogenic cardiomyopathy features. *JACC Clin Electrophysiol*. 2020;6(11):1353-1363. doi:10.1016/j.jacep.2020.05.026
 77. Sendfeld F, Selga E, Scornik FS, Pérez GJ, Mills NL, Brugada R. Experimental models of Brugada syndrome. *Int J Mol Sci*. 2019;20(9):2123. doi:10.3390/ijms20092123
 78. Gillette K, Gsell MAF, Strocchi M, et al. A personalized real-time virtual model of whole heart electrophysiology. *Front Physiol*. 2022;13:907190. doi:10.3389/fphys.2022.907190
 79. Pathmanathan P, Gray RA. Validation and trustworthiness of multiscale models of cardiac electrophysiology. *Front Physiol*. 2018;9:325032.
 80. Boukens BJ, Christoffels VM, Coronel R, Moorman AF. Developmental basis for electrophysiological heterogeneity in the ventricular and outflow tract myocardium as a substrate for life-threatening ventricular arrhythmias. *Circ Res*. 2009;104(1):19-31. doi:10.1161/CIRCRESAHA.108.188698
 81. Boukens BJ, Sylva M, de Gier-de Vries C, et al. Reduced sodium channel function unmasks residual embryonic slow conduction in the adult right ventricular outflow tract. *Circ Res*. 2013;113(2):137-141. doi:10.1161/CIRCRESAHA.113.301565
 82. Miles C, Westaby J, Ster IC, et al. Morphometric characterization of collagen and fat in normal ventricular myocardium. *Cardiovasc Pathol*. 2020;48:107-224. doi:10.1016/j.carpath.2020.107224
 83. Kelly A, Salerno S, Connolly A, et al. Normal interventricular differences in tissue architecture underlie right ventricular susceptibility to conduction abnormalities in a mouse model of Brugada syndrome. *Cardiovasc Res*. 2018;114(5):724-736. doi:10.1093/cvr/cvx244
 84. Boukens BJ, Remme CA. Intramural clefts and structural discontinuities in Brugada syndrome: the missing gap? *Cardiovasc Res*. 2018;114(5):638-640. doi:10.1093/cvr/cvy028
 85. Caloe K, Aistrup GL, Di Diego JM, Goodrow RJ, Treat JA, Cordeiro JM. Interventricular differences in sodium current and its potential role in Brugada syndrome. *Physiol Rep*. 2018;6(14):e13787. doi:10.14814/phys2.13787
 86. Biasi N, Tognetti A. A computationally efficient dynamic model of human epicardial tissue. *PLoS One*. 2021;16(10):e0259066. doi:10.1371/journal.pone.0259066
 87. Biasi N, Seghetti P, Tognetti A. Diffuse fibrosis and repolarization disorders explain ventricular arrhythmias in Brugada syndrome: a computational study. *Sci Rep*. 2022;12(1):8530. doi:10.1038/s41598-022-12239-9
 88. Ten Tusscher KHWJ, Panfilov AV. Wave propagation in excitable media with randomly distributed obstacles. *Multiscale Model Simul*. 2005;3(2):265-282. doi:10.1137/030602654.21
 89. Sarcon A, Hsia H, Postema PG, et al. Fractionated epicardial electrograms. *JACC Clin Electrophysiol*. 2021;7(2):258-270. doi:10.1016/j.jacep.2020.12.009
 90. Hoogendijk MG, Potse M, Vinet A, de Bakker JMT, Coronel R. ST segment elevation by current-to-load mismatch: an experimental and computational study. *Heart Rhythm*. 2011;8(1):111-118. doi:10.1016/j.hrthm.2010.09.066
 91. Behr ER, Ben-Haim Y, Ackerman MJ, Krahn AD, Wilde AAM. Brugada syndrome and reduced right ventricular outflow tract conduction reserve: a final common pathway? *Eur Heart J*. 2021;42(11):1073-1081. doi:10.1093/eurheartj/ehaa1051
 92. Alonso S, Bär M. Reentry near the percolation threshold in a heterogeneous discrete model for cardiac tissue. *Phys Rev Lett*. 2013;110(15):158-101. doi:10.1103/PhysRevLett.110.158101
 93. Wülfers EM, Moss R, Lehrmann H, et al. Whole-heart computational modelling provides further mechanistic insights into ST-segment elevation in Brugada syndrome. *Int J Cardiol Heart Vasc*. 2024;51:101373. doi:10.1016/j.ijcha.2024.101373
 94. Hoogendijk MG, Potse M, Linnenbank AC, et al. Mechanism of right precordial ST-segment elevation in structural heart disease: excitation failure by current-to-load mismatch. *Heart Rhythm*. 2010;7(2):238-248. doi:10.1016/j.hrthm.2009.10.007
 95. Veltmann C, Papavassiliu T, Konrad T, et al. Insights into the location of type I ECG in patients with Brugada syndrome: correlation of ECG and cardiovascular magnetic resonance imaging. *Heart Rhythm*. 2012;9(3):414-421. doi:10.1016/j.hrthm.2011.10.032
 96. Daw JM, Chahal CAA, Arkles JS, et al. Longitudinal electrocardiographic assessment in Brugada syndrome. *Heart Rhythm O2*. 2022;3(3):233-240. doi:10.1016/j.hroo.2022.01.011
 97. Richter S, Sarkozy A, Veltmann C, et al. Variability of the diagnostic ECG pattern in an ICD patient population with Brugada syndrome. *J Cardiovasc Electrophysiol*. 2009;20(1):69-75. doi:10.1111/j.1540-8167.2008.01282.x
 98. Gray B, Kirby A, Kabunga P, et al. Twelve-lead ambulatory electrocardiographic monitoring in Brugada syndrome: potential

- diagnostic and prognostic implications. *Heart Rhythm*. 2017;14(6): 866-874. doi:10.1016/j.hrthm.2017.02.026
99. Miles C, Boukens BJ, Scrocco C, et al. Subepicardial cardiomyopathy: a disease underlying J-wave syndromes and idiopathic ventricular fibrillation. *Circulation*. 2023;147(21):1622-1633. doi:10.1161/CIRCULATIONAHA.122.061924
100. Weiss JN. Arrhythmias in Brugada syndrome. *JACC Clin Electrophysiol*. 2021;7(2):271-272. doi:10.1016/j.jacep.2020.12.020
101. Boukens BJ, Nademanee K, Coronel R. Reply: J-Wave syndromes: where's the scar? *JACC Clin Electrophysiol*. 2020;6(14):1863-1864. doi:10.1016/j.jacep.2020.10.003.22
102. Hoogendijk MG, Opthof T, Postema PG, Wilde AAM, de Bakker JMT, Coronel R. The Brugada ECG pattern: a marker of channelopathy, structural heart disease, or neither? Toward a unifying mechanism of the Brugada syndrome. *Circ Arrhythm Electrophysiol*. 2010;3(3): 283-290. doi:10.1161/CIRCEP.110.937029
103. Seghetti P, Biasi N, Tognetti A. A 3D transmurally heterogeneous computational model of the Brugada Syndrome phenotype. *IEEE Access*. 2023;11:81711-81724. doi:10.1109/ACCESS.2023.3301461
104. Renard E, Haïssaguerre M, Bernus O. Reply: the mechanism of brugada syndrome: is it induced only by conduction disturbance? *JACC Clin Electrophysiol*. 2023;9(11):2357. doi:10.1016/j.jacep.2023.09.008
105. Haïssaguerre M, Nademanee W, Hocini M, et al. The spectrum of idiopathic ventricular fibrillation and J-wave syndromes: novel mapping insights. *Card Electrophysiol Clin*. 2019;11(4):699-709. doi:10.1016/j.ccep.2019.08.011

How to cite this article: Seghetti P, Latrofa S, Biasi N, et al. Electrophysiological patterns and structural substrates of Brugada syndrome: Critical appraisal and computational analyses. *J Cardiovasc Electrophysiol*. 2024;1-15. doi:10.1111/jce.16341